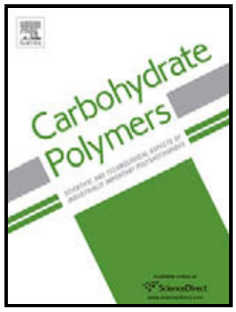

Title: Nanohybrid Hydrogels of Laponite: PVA-Alginate as a potential wound healing material

Authors: Nasim Golafshan, R. Rezahasani, M. Tarkesh Esfahani, M. Kharaziha, S.N. Khorasani

PII: S0144-8617(17)30946-3
DOI: http://dx.doi.org/10.1016/j.carbpol.2017.08.070
Reference: CARP 12677

To appear in:

Received date: 8-6-2017
Revised date: 15-8-2017
Accepted date: 15-8-2017

Please cite this article as: Golafshan, Nasim., Rezahasani, R., Tarkesh Esfahani, M., Kharaziha, M., & Khorasani, S.N., Nanohybrid Hydrogels of Laponite: PVA-Alginate as a potential wound healing material.*Carbohydrate Polymers* http://dx.doi.org/10.1016/j.carbpol.2017.08.070

Nanohybrid Hydrogels of Laponite: PVA-Alginate as a potential wound healing material

Nasim Golafshan[1], R. Rezahasani[2], M. Tarkesh Esfahani[3], M. Kharaziha[1*], S.N. Khorasani[2]

1. Department of Materials Engineering, Isfahan University of Technology, Isfahan 84156-83111, Iran

2. Department of Chemical Engineering, Isfahan University of Technology, Isfahan 84156-83111, Iran

3.Department of New Sciences and Technologies, University of Tehran, Tehran 1417466191, Iran

* **Corresponding author e-mail**: ma.kharaziha@gmail.com

Highlights

- • Nanohybrid hydrogel of Laponite:PVA-Alginate was synthesized for wound healing process.
- • Laponite were applied to enhance mechanical and cellular response of hybrid hydrogel
- • Laponite as hemostasis agent could decrease the coagulation time
- • Laponite nanoplatelets reduced the degradation rate of nanohybrid hydrogel

Abstracts

The aim of this study was to develop a novel nanohybrid interpenetrating network hydrogel composed of laponite:polyvinyl alcohol (PVA)-alginate (LAP:PVA-Alginate) with adjustable mechanical, physical and biological properties for wound healing application. Results demonstrated that compared to PVA-Alginate, mechanical strength of LAP:PVA-Alginate significantly enhanced (upon 2 times). Moreover, incorporation of 2 wt.% laponite reduced

swelling ability (3 times) and degradation ratio (1.2 times) originating from effective enhancement of crosslinking density in the nanohybrid hydrogels. Furthermore, nanohybrid hydrogels revealed admirable biocompatibility against MG63 and fibroblast cells. Noticeably, MTT assay demonstrated that fibroblast proliferation significantly enhanced on 0.5 wt.% LAP:PVA-alginate compared to PVA-alginate. Moreover, hemolysis and clotting tests indicated that the nanohybrid hydrogels promoted hemostasis which could be helpful in the wound dressing. Therefore, the synergistic effects of the nanohybrid hydrogels such as superior mechanical properties, adjustable degradation rate and admirable biocompatibility and hemolysis make them a desirable candidate for wound healing process.

Key words: Laponite; Interpenetrating network; polyvinyl alcohol; alginate; Hemorrhage; Wound healing applications

1. Introduction

Hydrogels as extremely hydrophilic macromolecular networks are attractive candidates for wound healing process (Lee & Mooney, 2001). The principal goal of wound healing is to prompt recovery of damaged tissue with negligible scarring and maximal regeneration. In this way, the wound dressing membranes need to have essential characteristics to support wound healing and keep the damaged site from contamination. For wound healing process, hydrogel dressings should preserve a humid environment around the wound and retain the wound exudates encouraging fibroblast proliferation and keratinocyte migration (Jhong et al., 2014). The formation of clot is one of the crucial processes for wound healing which establish hemostasis by concentrating clotting factors and forming a physical barrier against bleeding (Gaharwar et al., 2014). However, applications of hydrogels have often been limited due to their inadequate mechanical strength and toughness as well as high degradation rate (Annabi et al., 2014).

Numerous strategies have been proposed to develop hydrogels with superior mechanical properties. Hydrogels with excellent mechanical characteristics could be categorized into three

main types consisting of topological (TP), nanocomposite (NC) and double network (DN) gels (Haraguchi & Takehisa, 2002; Tanaka, Gong, & Osada, 2005). Between them, DN gels are 3D networks comprising of two or more interpenetrating polymer networks (IPN), partly or entirely intertwined on a molecular scale, (Hoare & Kohane, 2008). IPNs afford both mechanical strength and toughness when one component is cross-linked covalently, and another one is ionically cross-linked (Naficy, Kawakami, Sadegholvaad, Wakisaka, & Spinks, 2013). Recently, various hybrid ionic-covalent IPN hydrogels have been developed consisting of polyacrylamide (PAAm)- alginate (Darnell et al., 2013), poly(acrylic acid) (PAA)-alginate (Lin, Ling, & Lin, 2009) and polyvinyl alcohol (PVA)-Alginate (Golafshan, Kharaziha, & Fathi, 2016; Thankam, Muthu, Sankar, & Gopal, 2013). Due to the cytocompatibility, hydrophilicity, water solubility, suitable mechanical properties as well as low price, PVA has been widely applied for engineering various tissues such as bone (Nie et al., 2012), heart (Thankam et al., 2013), nerve (Golafshan et al., 2016) and vascular network (L. V. Thomas, Arun, Remya, & Nair, 2009). Moreover, alginate is a negatively charged polysaccharide derived from brown seaweed, which has been widely applied to develop IPN hydrogels. Due to non-toxicity, biodegradability and biocompatibility, alginate has been extensively applied for tissue engineering application (Wong, 2004) and cell therapy (Orive, Tam, Pedraz, & Hallé, 2006). Moreover, alginate gels and sponges have been applied as wound dressings and treatments due to their ability to improve healing rate and cellular activity characteristics of wound such as haemostatic, adhesion and cell proliferation. Results showed that addition of alginate in PVA-alginate membranes enhanced swelling capability, and *in vitro* protein adsorption. However, alginate reduced mechanical stability of membranes (Lee & Mooney, 2012). Tarun *et al.* (Tarun & Gobi, 2012) found that PVA-alginate fibrous membranes with high alginate content revealed high water vapor

transmission property, providing the moist environment leading to wound healing acceleration.

Recently, nanohybrid hydrogels consisting of various kinds of nano-fillers such as graphene, hydroxyapatite, carbon nanotubes and metallic nanoparticles have gained importance for tissue engineering and wound healing applications (Kharaziha et al., 2014; Riedinger et al., 2011). Between them, nanoclays are the well-established components for drug delivery, tissue engineering and wound healing applications (P. Li, Kim, Hui, Rhee, & Lee, 2009; Pacelli et al., 2016; Roozbahani, Kharaziha, & Emadi, 2017). The commonly used nanoclays is montmorillonite, hectorite, and smectite family (Wu, Gaharwar, Schexnailder, & Schmidt, 2010). The smectite family of clays is hydrous materials, which swell after absorbing water and form plastic mass with strong adhesiveness. Among the smectite family, laponite, $Na_{0.7}[(Mg_{5.5}Li_{0.3})Si_8O_{20}(OH)_4]_{0.7}$, is a synthetic nanoclay consisting of a layered structure with 30 nm diameter and 1 nm in thickness (Wu, Gaharwar, Chan, & Schmidt, 2011). The unique properties of laponite such as high biocompatibility, anisotropic and plate-like morphology and great surface area along with its great ability to cationic exchange make it a promising material for the improvement of numerous physical and mechanical characteristics of hydrogels in various forms (P. Li, Kim, Yoo, & Lee, 2009; H. Yang, Hua, Wang, & Wang, 2011). One of the most and interesting properties of smectite nanoclays, specifically laponite, is their blood clotting ability. Laponite can absorb water in blood and concentrate the cells and clotting factors leading to promote hemostasis (Arnaud et al., 2009; Bowman, Wang, Meledeo, Dubick, & Kheirabadi, 2011). Gaharwar *et al.* (Gaharwar et al., 2014) has recently developed shear-thinning hydrogel composed of laponite and gelatin as an injectable hemostatic agent with 77% reduced blood-clotting time compared to gelatin. According to our knowledge, the combination of laponite

nanoplatelets and IPN hydrogels of PVA-alginate as a wound dressing material have never been studied.

The objective of this work was to develop nanohybrid IPN hydrogels of laponite incorporated PVA-Alginate (LAP:PVA-Alginate) and study the effects of laponite concentration (0, 0.5, 1 and 2 wt.%) on the physical, mechanical and biological properties of nanohybrid hydrogels. It is hypothesize that incorporation of laponite nanoplatelets within IPN hydrogels of PVA-Alginate may provide nanohybrid hydrogels with appropriate mechanical, physical and biological characteristics for wound healing application. Moreover, it is expected that the addition of laponite nanoplatelets may result in the improved hemostasis properties of nanohybrid hydrogel, which could be helpful to control the bleeding of wound site.

2. Materials and methods

2.1. Materials

Alginic acid sodium salt (SA) from brown algae (Mw range of 80,000-120,000 and with approximate mannuronic/guluronic ratio of 1.56) and PVA (Mw=72,000) were purchased from Sigma, St. Louis, MO, USA. $CaCl_2$ and methanol were obtained from Merck Chemicals, USA. Synthetic silicate nanoplatelets (Laponite RDS) containing SiO_2 (59.5%), MgO (27.5%), Na_2O (2.8%) and Li_2O (0.8%) with low heavy metals content were purchased from Rockwood Additives Limited, UK. Deionized (DI) water was used in all the sections of the experiment.

2.2. Fabrication of nanohybrid hydrogel of LAP:PVA-Alginate

Nanohybrid hydrogels of LAP:PVA-Alginate with various concentrations of laponite (0, 0.5, 1 and 2 wt.% of prepolymer) were prepared using gel casting technique. Primarily, separate alginate and PVA aqueous solutions with the concentration of 4 and 10 wt.% were prepared,

respectively. After stirring at 60 °C overnight, two solutions were mixed at the weight ratio of 1:1 at room temperature for 2 h to get a homogenous solution. Consequently, various amounts of laponite nanoplatelets (0, 0.5, 1, and 2 wt.%) were dispersed in 2 ml DI water and sonicated for 30 min (WUDD10H, Power 770 W), two times. Following the addition of laponite suspension to the above polymeric solution, the suspensions were mixed at 60 °C for 2 h and sonicated for 30 min, to provide a homogenous dispersion of laponite nanoplatelets. Finally, after degassing, the suspensions were transferred into Petri-dish and maintained for 24 h to be completely polmerized. It should be noted that, before casting, the cylindrical glass mold was sprayed with Teflon (Welcon co) for surface lubricant. Consequently, hydrogels were removed from the molds and were covalently and ionically crosslinked, respectively. Initially, the hydrogels were maintained at 80 °C for 24 h, and then, dipped in absolute methanol solution for 24 h to crosslink PVA. Consequently, the samples were immersed in 2 wt.% $CaCl_2$ solution for 24 h at room temperature to ionically crosslink alginate. Consequently, uncrosslinked polymers were removed by three-times rinsing the samples in phosphate buffered saline (PBS, pH=7.4) solution. It should be noted that, according to the concentration of laponite nanoplatelets (0, 0.5, 1, and 2 wt.%), nanohybrid hydrogels were named as PVA-Alginate, 0.5LAP:PVA-Alginate, 1LAP:PVA-Alginate and 2LAP:PVA-Alginate, respectively.

2.3. Characterization of nanohybrid hydrogel of LAP:PVA-Alginate

The chemical composition of the nanohybrid hydrogels was verified through X-ray diffraction (XRD, X' Pert Pro X-ray diffractometer, Phillips, Netherlands) technique carried out with monochromatized CuKa radiation ($\lambda = 0.154$ nm) at a generator voltage of 40 kV. Moreover, attenuated total reflectance-Fourier transform infrared spectroscopy (ATR-FTIR, Bruker tensor) performed over a range of 600-3700 cm^{-1} and resolution of 2 cm^{-1} was used to

determine the chemical composition and IPN formation. Furthermore, the distance between the laponite's layers purely and in 2LAP:PVA-Alginate was analyzed using XRD patterns using Bragg's equation (Eq. 1):

$$d = \frac{\lambda}{2Sin\theta} \quad (1)$$

In which λ is the wavelength of the copper anode source (0.154 nm), d stands for the spacing between the scattering laponite's layers, and θ is the diffraction angle.

The surface morphology of the nanohybrid hydrogels as well as the distribution of laponite nanoplatelets within the IPN hydrogels was evaluated by using scanning electron microscope (SEM, Philips, XL30). Before imaging, the samples were sputter coated with a thin layer of gold. Moreover, the transmission electron microscopy (TEM, Leo 912AB) was utilized to characterize the morphology of the laponite nanoplatelets.

The swelling behavior of hybrid hydrogels was investigated in PBS at 37 °C and pH=7.4, at the predetermined time intervals. The samples were accurately weighted and immersed in PBS. After removing the samples from PBS and blotting off excess PBS, the wet mass of samples was measured. The swelling rate was calculated according to the following equation (Eq. 2):

$$\%Swelling\ ratio = \frac{(M_{wet} - M_{int})}{M_{int}} \times 100 \quad (2)$$

where W_{wet} and W_{int} were the mass of the swollen and dried samples, respectively. In vitro degradation rate of samples was investigated by monitoring the weight loss over 28 days of incubation in PBS (pH=7.4). Three samples of each type of nanohybrids with the weight of around 10 mg were incubated in PBS at 37 °C. At each specific time point (7, 14, 21 and 28 days), the samples were washed with PBS, dried and weighted. Ultimately, the degradation rate was assessed via dividing the weight loss by the initial dry weight.

Tensile properties of the samples were determined by a Hounsfield H25KS tensile tester, using a load cell capacity of 10 N and rate of 2 mm. min^{-1}. The samples were cut in the rectangular shapes with the dimension of about 10 mm×30 mm×500 µm. The mechanical test was performed in the wet condition and room temperature. Therefore, before mechanical testing, the samples were soaked in PBS for 2h. Finally, the stress-strain curves (n=5) were plotted and the mechanical characteristics consisting of tensile strength, elastic modulus and toughness were estimated.

2.4. Cell Culture

The cytotoxicity of LAP:PVA-Alginate sample was considered based on by 3-(4,5-dimethylthiazolyl-2)-2,5-diphenyl tetrazolium bromide (MTT) assay using two cell lines consisting of human dermal fibroblasts and MG63 cell lines from the National Cell Bank of Iran at the Pasteur Institute. Before cell seeding, fibroblasts and MG63 cells were cultured in full medium of Dulbecco's Modified Eagle Medium (DMEM-low, Bioidea, Iran) consisting of 10 (v/v)% fetal bovine serum (FBS) (Bioidea, Iran) and 1 (v/v)% streptomycin/ penicillin (Bioidea, Iran) at 37 °C and 5% CO_2 condition. Before cell culture, the samples were placed in a 48-well plate, rinsed with PBS (pH=7.4) and, finally, sterilized for 1 h in 70 (v/v)% ethanol and 2 h ultraviolet light. Afterward, the samples were immersed in full medium overnight. After reaching 70-80% confluency, two cell types were detached with 0.25% trypsin/EDTA solution (Bioidea, Iran) and seeded on the nanohybrid samples (n=3) as well as tissue culture plate (TCP) (control) with a density of 10^4 cells per well, separately. Cells were incubated at 37 °C under 5% CO_2 for 7 days for fibroblasts and MG63 while the medium was changed every three days.

At the specific time points (1, 4 and 7 days of culture), the culture medium was removed and incubated with MTT solution (0.5 mg/ml MTT reagent in PBS) for 4 h. Consequently,

dimethyl sulfoxide (DMSO) was added to dissolve the purple MTT-formazan crystals and kept for 1 h at 37 °C. Finally, dissolved formazan solution of each sample was transferred to 96-well plate and the optical density (OD) of each well was measured with a microplate reader (Bio Rad, Model 680 Instruments) against DMSO (blank) at a wavelength of 490 nm. The relative cell viability was estimated based on the following equation (Eq. 3):

$$Relative\ cell\ viability\ (\%) = \frac{A_{sample} - A_c}{A_b - A_c} \quad (3)$$

Where A_{sample}, A_b and A_c stand for the absorbance of the sample, blank (DMSO) and control (TCP), respectively.

2.5. Protein adsorption

The adsorption of bovine serum albumin (BSA) on the surface of samples was investigated via batch contact method (C. Li, Mu, Lin, & Ngai, 2015). Briefly, pre-weighed hydrogels were immersed in PBS (pH=7.4) for 3 h to swell and then weighed. Consequently, the samples were soaked in 20 mL of 0.2 wt.% BSA solution (pH=7.4) and then were shaken for 30 min to prevent from the solution–air interface formation. As-prepared supernatants were analyzed to determine the residual BSA in solution using ultraviolet spectrophotometer at 280 nm. The amount of adsorbed protein (mg/ml) was calculated according to the following equation (Eq. 4):

$$\text{Adsorbed BSA (mg/g)} = \frac{C_0 - C_a}{w} V \quad (4)$$

where C_0 and C_a are the BSA concentrations (mg/mL) before and after adsorption, respectively, w is the weight of the swollen nanohybrid hydrogels (g) and V is the volume of the BSA solution (mL).

2.6. Hemolysis assay

Blood-nanohybrid interactions were estimated according to hemolysis and kinetic clotting

time assays. For both tests, healthy human blood drawn from healthy adult volunteer consisting of sodium citrate (3.8 wt. %) diluted with normal saline (4:5 volume ratio) was applied.

LAP:PVA-Alginate samples with size of 1 cm×1 cm×5 mm (n=3) were put into centrifuge tubes containing 10 mL of normal saline and incubated at 37 °C for 30 min. Following the addition of 200 µl diluted blood, the tubes were incubated for 60 min at 37 °C. Subsequently, the tubes were centrifuged for 5 min at 2700 rpm, and the supernatants were removed. Finally, the absorbance of the solutions was measured with ultraviolet spectrophotometer at 540 nm and the hemolysis ratio (HR) was calculated according to the following equation (Eq. 5) (Zou et al., 2016):

$$\%HR = \left(\frac{A_{sample} - A_n}{A_p - A_n}\right) \times 100 \quad (5)$$

where A_{sample}, A_p, and A_n represent the absorbance of samples, the positive control (distilled water) and the negative control (normal saline), respectively.

2.7. Kinetic clotting test

To evaluate kinetic clotting property, the hydrogels (n=3) were placed at the small vials containing diluted blood and was kept in the incubator at 37 °C. At the specific time points (5, 20, 35, 50, 90, and 130 min), the hydrogels were washed with 50 ml distilled water to provide disemboguement samples. Finally, absorbance of the samples was estimated at 540 nm using a microplate reader and the OD values were reported.

2.8. Statistical analysis

One-way ANOVA (n≥3) was applied for statistical analysis. To establish a statistical significance difference between groups, Tukey's post-hoc test using GraphPad Prism Software (V.6) with a p-value <0.05 was applied to be significant.

3. Results and discussion

3.1. Solid-state characterization of LAP: PVA-Alginate hydrogels

3.1.1. Physical and chemical characterization

Due to hydrophilic nature, sufficient flexibility and ability to control the lost fluids from the body, hydrogels have been widely applied for dressing membranes. However, their weak mechanical stability has limited their applications. To overcome these issues, various types of hybrid hydrogels have been developed from a range of materials (Annabi et al., 2010). In this research, this weakness was addressed by two different strategies consisting of formation of IPN hydrogels and nanohybrid hydrogels using laponite nanoplates as nano-fillers. According to Fig. 1A, hybrid IPN hydrogel was developed using a combination of two polymers of covalently – crosslinked PVA and ionically-crosslinked sodium alginate and incorporation of laponite within the polymer matrix. The formation of IPN was confirmed using FTIR spectroscopy. FTIR spectra of crosslinked PVA and alginate (Fig. 1B) and their characteristic bands (supplementary Table S1) were similarly reported in previous researches, confirming the crosslinking of these two polymers (Broderick et al., 2006; Golafshan et al., 2016). FTIR spectrum of crosslinked PVA-Alginate consisted of both characteristic bands of crosslinked alginate and PVA with slight differences consisting of reduced intensity of some characteristic peaks related to PVA (840 cm^{-1}, 1090 cm^{-1}, 1325 cm^{-1}, and 1427 cm^{-1}) and disappearance of other bands (at 1250 cm^{-1}, 1370 cm^{-1}, and 1733 cm^{-1}) due to the interaction between PVA and alginate. Moreover, the hydroxyl-stretching band (O-H) of alginate became broader after formation of PVA-Alginate hydrogel. This behavior strongly supported the idea that hydrogen bonding formed between the hydroxyl groups of PVA and that of alginate (Islam & Karim, 2010; Shalumon et al., 2011). This interaction is schematically shown in Fig. 1A confirming the formation of the semi-interpenetrating network of PVA and alginate. By immersing the hydrogels in calcium content

solutions, the calcium ions replaced the sodium ions of alginate structure in the polymer chain and attach to two of the polymer strands leading to the ionically crosslinking of the hydrogel network. Upon heat treatment and methanol exposure, PVA chains of PVA-alginate hydrogel covalently crosslinked together and hydrogen bonding was formed with ionically crosslinked alginate chains which may enhance the mechanical and physical properties of IPN hydrogels.

To develop nanohybrid hydrogels, laponite nanoplatelets consisting of plate-like particles with average size of 47.3±10 nm (Fig. 1C) were incorporated within IPN matrix (Fig. 1A). FTIR spectrum of laponite (Fig. 1B) and its characteristic bands (Supplementary Table S1) showed the presence of distinctive absorption bands which were similarly reported in previous researches (Mahdavinia, Mousanezhad, Hosseinzadeh, Darvishi, & Sabzi, 2016). Furthermore, FTIR spectrum of 2LAP:PVA-Alginate consisted of the characteristic bands of laponite and crosslinked PVA and alginate with some differences. For instance, the intensity of the bonds at 2918 and 2846 cm^{-1} which were related to CH stretching vibration, reduced. Moreover, some other peaks at 3600 and 1040 cm^{-1} shifted to lower wavenumbers and became broader. The slight broadening of the hydroxyl band in the 2LAP:PVA-Alginate might be due to inter-molecular hydrogen interactions between PVA-alginate chains and laponite (Auvray & Lal, 1999; Loizou et al., 2005; Shubhangi H Nair, Kiran C Pawar, Jyoti P Jog, & Manohar V Badiger, 2007). Furthermore, compared to FTIR spectrum of laponite, Si-O-Si stretching vibration shifted slightly towards the higher frequency side (1022 cm^{-1}) which can be attributed to the interactions between PVA-Alginate polymer network and laponite through Si-OH groups. This result strongly confirmed that laponite nanoplatelets acted as physical crosslinker for further

crosslinking of polymer chains (Shubhangi H. Nair, Kiran C. Pawar, Jyoti P. Jog, & Manohar V. Badiger, 2007).

XRD pattern of 2LAP:PVA-Alginate confirmed the presence of laponite nanoplatelets within PVA-Alginate matrix (Fig. 1D). XRD patterns of crosslinked PVA and alginate hydrogels exhibited broad and weak diffraction peaks due to the strong intermolecular and intra-molecular hydrogen bonding between polymer chains after crosslinking process. XRD pattern of PVA-Alginate hydrogel, after crosslinking process, revealed disappearance of the peaks corresponding to both polymers and formation of one new broad peak at around 2Θ=19.6° demonstrating the interaction between alginate and PVA. XRD pattern of laponite consisted of the characteristic diffraction peaks at 2θ =19.6°, 27.6° and 35.4° related to (02,11), (005), (20,13) diffractions, respectively, which were similarly reported in previous researches (Guimarães, Ciminelli, & Vasconcelos, 2007; Wang et al., 2012). After mixing laponite nanoplatelets with PVA-Alginate blend and crosslinking process, the sharp peaks in the XRD pattern related to laponite slightly shifted to 2θ =34.6° due to the formation of hydrogen bonds between laponite and PVA-Alginate blend. The d-spacing parameter of laponite nanosheets was calculated before and after hybrid formation and confirmed the well dispersion of laponite within the polymer matrix. The d-spacing parameter for the interlayer distance in the laponite nanoplates at 2θ = 35.4° and 2LAP:PVA-Alginate at 2Θ=34.6° (corresponded to (20,13) plane) were estimated about 0.25 nm and 0.26 nm, respectively. This result confirmed that the polymer chains placed between laponite nanoplatelets and changed the lattice parameter of laponite. Other authors also reported similar conclusions (Jung, Kim, Choy, Hwang, & Choy, 2008).

SEM images of the hydrogels (Fig. 2) confirmed that the distribution of laponite nanoplatelets within PVA-Alginate matrix depended on the laponite concentration (0, 0.5, 1 and

2 wt.%). While the surface of PVA-Alginate was smooth, 0.5LAP:PVA-Alginate hydrogel consisted of laponite nanoplatelets exfoliated and uniformly dispersed throughout the polymer matrix without any large agglomeration. Incorporation of more laponite nanoplatelets, especially at 2LAP:PVA-Alginate, led to the agglomeration of laponite nanoplatelets, which might be resulted in reduced mechanical properties of the hydrogels. The effect of nanoparticle distribution on the improvement of nanohybrid properties such as mechanical, biological and hemolysis due to the strong interaction between filler and matrix was similarly reported, previously (Gaharwar et al., 2014; Gaharwar et al., 2010).

3.1.2. Swelling and degradation evaluation

One of the undeniable characteristics of dressing materials, which determine their effectiveness, is swelling capacity. Dressing materials need to show optimized level of fluid absorption ability in order to eliminate extreme exudates. Moreover, as the main function of exudate is to help the diffusion of healing factors such as growth factors and to promote keratinocyte migration and fibroblast proliferation, actual exudate organization could decrease healing time, diminish exudate-related issues and, overall, improve healthcare effectiveness (S. Thomas, 1997). Therefore, application of dressing materials with ability to moderately absorb fluid could be beneficial in wound healing. The swelling property of hydrogels, consisting of various amounts of laponite nanoplatelets, after immersion in PBS (pH 7.4) for 24 h is presented in Fig. 3A. It was concluded that all hydrogels revealed similar swelling ability with different amplitudes. The swelling ratio of nanohybrid hydrogels significantly enhanced at the early stage, and then reached to the steady state condition. It was realized that, incorporation of laponite noticeably diminished their swelling ability. For instance, after 24 h soaking, the swelling ratio of PVA-Alginate decreased 3.2 times from 274.6±6.5% (for PVA: Alginate) to

85.9±2.6% (for 2LAP:PVA-Alginate). Several parameters affect the swelling rate of nanohybrids, such as the hydrophilic ability of nanoparticles, structure of polymer network, and the interaction between polymer chains and nanoparticles (Mahdavinia, Ettehadi, Amini, & Sabzi, 2015). According to the results of FTIR spectroscopy, reduced swelling ratio of hybrid hydrogels could be due to the fact that incorporation of laponite acted as an additional physical crosslinker in the hybrid hydrogel preventing from water absorption. Such this finding was reported in other researches where laponite nanoplatelets revealed the significant effect on the swelling ratio of poly(ethylene glycol) (PEG)-poly(trimethylene carbonate) (PTMC) (Mahdavinia et al., 2016; Sharifi, Blanquer, van Kooten, & Grijpma, 2012).

One of the most important properties of materials for wound healing process is their degradation rate. The degradation rate of hydrogels indirectly affects cell function and remodeling of the host tissue. Previous results confirmed that the strategy by which cells infiltrate and migrate through the hydrogel matrix could be related to its degradation (Vu, Jain, Veres, & Rajagopalan, 2014). Fig. 3B shows that while degradation profile of LAP:PVA-Alginate hydrogels was similar to that of PVA-Alginate, the slop of these profiles varied depending on the laponite concentration. With an increase in laponite nanoplatelets in the nanohybrid hydrogels, degradation rate of the hydrogels significantly reduced from 67.1±1.9% (for PVA-Alginate) to 64.80±1.2% (for 0.5LAP:PVA-Alginate), 57.8±2.3% (for 1LAP:PVA-Alginate) and 54.1±3.6% (for 2LAP:PVA-Alginate), after 28 days of soaking. The slower degradation rate of LAP:PVA-Alginate hydrogels compared to PVA-Alginate might be due to the presence of laponite which acted as a additional crosslinker between polymer chains. Therefore, hydrophilic chains of PVA-Alginate were less accessible to the hydrolyzing medium

leading to the reduced degradation rate of LAP:PVA-Alginate compared to PVA-Alginate hydrogel.

3.1.3. Mechanical characterization

The main disadvantage of hydrogels in would healing process is improper mechanical stability and weak mechanical strength (Hoffman, 2012). It has been described that incorporation of nanomaterials such as nanoclays within hydrogel matrix is an effective and simple way to enhance the stability of hydrogels (Cha et al., 2014). To evaluate the effects of laponite nanoplatelets on the mechanical properties of PVA-Alginate hydrogel, uniaxial tensile test was performed. Before mechanical testing, the samples were submerged in PBS (pH=7.4) for 2h. Fig. 4 confirmed that incorporation of laponite nanoplatelets resulted in the formation of relatively robust hydrogel with controlled flexibility. Fig. 4A shows tensile stress–strain curves of PVA-Alginate nanohybrid hydrogels consisting of various amounts of laponite nanoplatelets. The hydrogels exhibited an elastic region followed by a plastic region after yielding. In the elastic region, the stress increased almost linearly with the strain followed by nonlinear behavior before the maximum stress. The mechanical properties of the hydrogels, extracted from the curves, are presented in Fig.4B-D. Results confirmed the effective role of laponite concentration on the mechanical properties of the hydrogels. For instance, it was found that addition of 0.5 wt.% laponite dramatically improved toughness (2.5 times), strength (1.7 times), and tensile modulus (2.7 times) compared to PVA-Alginate hydrogel. It might be related to the effective interaction between the polymer matrix and laponite nanoplatelets and extra-crosslinking of the matrix with nanoplatelets. Such these findings were reported in another research (Mahdavinia et al., 2016). As depicted in Fig.4F, after crosslinking process, the IPN hydrogel was formed due to the hydrogen bonding between the chains of two polymers. After incorporation of laponite

nanoplatelets within IPN hydrogel, the interaction between the laponite surface and functional groups of polymers resulted in significant load transfer to laponite nanoplatelets and improved tensile strength. Nevertheless, incorporation of more laponite content upon 2 wt.% led to significantly reduced mechanical properties. It might be attributed to the agglomeration of laponite nanoplatelets leading to the weak interaction between laponite nanoplatelets and PVA-Alginate matrix. Such result was similarly demonstrated in the laponite-poly(acrylic acid) nanocomposite at high clay concentrations (Du et al., 2015). Result showed that the maximum strength (308 kPa) was achieved at 0.14 wt.% laponite content. In another research, the effects of laponite concentration and chemical crosslinking on the mechanical properties of polyacrylamide were investigated (J. Yang et al., 2016). Hybrid polyacrylamide/laponite nanocomposite gels exhibited better fracture stress, elastic modulus, and fracture energies than those of polyacrylamide gel. Our results confirmed that incorporation of 0.5 wt.% laponite nanoplatelets within PVA-Alginate was highly useful to improve mechanical properties of the hybrid hydrogels, especially toughness. This property could allow the dressings to fit well in the wound sites making it useful for wound healing application.

3.2. Biological evaluation of LAP: PVA-Alginate hydrogels

3.2.1. Cytotoxicity study

A wound dressing hydrogel should provide a favorable microenvironment to improve cellular activity property of wound such as haemostatic, adhesion and cell migration and proliferation (Kamoun, Kenawy, & Chen, 2017). MTT assay (Fig. 5) demonstrated that the proliferation of fibroblasts and MG63 cells seeded on the hydrogels gradually enhanced from day 1 to day 7. For instance, the proliferation of fibroblasts (Fig. 5A) cultured on PVA-Alginate hydrogel improved from 71.2±7.2 %(control) (at day 1) to 86.7±3.9%(control) (at day7).

Moreover, the proliferation of fibroblasts on LAP:PVA-Alginate hydrogels improved and reached the highest value on 0.5LAP:PVA-Alginate. For instance, after 7 days of culture, the proliferation of fibroblast cells on 0.5LAP:PVA-Alginate (125.1±4.6%(control)) significantly enhanced (1.5 times) compared to that of on the PVA-Alginate (86.7±3.9 % control) ($p<0.05$).

Moreover, according to Fig. 5B, the proliferation of MG63 cells seeded on the hydrogels gradually enhanced from day 1 to day 7. This observation reflected the cell-compatibility of the hydrogels and confirmed nontoxicity of crosslinking treatment. While the proliferation of MG63 cells after 7 days of culture on PVA-Alginate hydrogel was 97.8±4.6%(control), incorporation of 0.5 wt.% significantly promoted it (1.8 times) to 179.5±20.6%(control) ($p<0.05$). However, incorporation of more laponite content upon 2 wt.% resulted in considerably reduced proliferation ratio compared to 0.5LAP:PVA-Alginate at day 7 ($p<0.05$). Along with previous researches, these results might be due to the effect of mechanical properties of nanohybrid hydrogels on the cell proliferation (Cai et al., 2016; Golafshan, Gharibi, Kharaziha, & Fathi, 2017).

PVA and alginate have been widely used for wound dressing due to their ability to support cell function. According to Fig. 5, nanohybrid hydrogels were found to be non-cytotoxic and laponite did not have unfavorable affect on the biocompatibility of PVA-Alginate matrix. Similar result was also reported for laponite-poly(ethylene glycol) hydrogel in contact with several cell types (Gaharwar, Dammu, Canter, Wu, & Schmidt, 2011; Gaharwar, Rivera, Wu, & Schmidt, 2011; Liu et al., 2014). This implied that the presence of laponite as a nano-filler not only improves the physical and mechanical characteristics of nanohybrid films, but also resulted in the improved cell proliferation rate due to the leachable ions from the degrading nanohybrid

hydrogel. When laponite nanoparticles dispersed in physiological solution, they released some inorganic ions such as $Mg^{2+,}$ Na^{+}, $Si(OH)_4$, and Li^{+} which stimulated cell viability. Among these ions, Mg^{2+} as a divalent cation resulted in enhanced cellular attachment to nanohybrid hydrogel surface which were facilitated primarily by protein bonding belonging to the integrin family (Eslahi, Simchi, Mehrjoo, Shokrgozar, & Bonakdar, 2016).

3.2.2. Protein adsorption

As the first step of thrombosis formation on the biomaterial surface is BSA adsorption, enhancement of BSA adsorption implies better thrombotic property. Therefore, the amount of adsorbed protein on the hydrogel surfaces was determined. According to Fig. 6A, the amount of adsorbed BSA enhanced with increasing laponite content within the nanohybrid hydrogels. The amount of adsorbed BSA on PVA-Alginate hydrogel was 2.2±0.3 mg/g, which was less than that of the laponite containing hydrogels. Noticeably, addition of laponite upon 2 wt.% to hybrid hydrogels resulted in the increased BSA adsorption capacity to 7.3±0.7 mg/g. It might be related to the hydrophilic nature and biocompatibility of polymer matrix, which reduced with increasing laponite content. Generally, the protein adsorption initiates with the hydration of the surface exposed to a protein containing solution and formation of a thin layer at the interface. Consequently, this layer replaced with adsorbing protein molecules and formation of a new 3D interphase. As interphase water is supported by surface-bound water through hydrogen bonds, displacement of adsorbed water at interphase strictly depends on the surface chemistry, which regulates the amount of adsorbed protein. In this way, as hydrophilicity of the surface increases, protein adsorption declines due to the enhanced energetic cost of surface dehydration (Vogler, 2012). Therefore, in agreement with previous results (Xu, Bauer, & Siedlecki, 2014), further BSA could be absorbed on the LAP:PVA-Alginate hydrogels than PVA-Alginate one which

might be attributed to easy displacement of protein with adsorbed water molecules and may lead to less anti-thrombogenic property.

3.2.3 In vitro whole blood-hydrogel interaction

Hemolysis assay was performed as an easy and trustworthy approach to evaluate blood compatibility of materials. Hemolysis assay is based on the degree of the erythrolysis and hemoglobin dissociation when the hydrogels are in contact with blood (C. Li et al., 2015). Fig. 6B shows the hemolysis ratio of LAP:PVA-Alginate samples as a function of laponite concentration. It was found that the hemolysis ratio of LAP:PVA-Alginate hydrogels enhanced with increasing laponite contents. For instance, the hemolysis ratio of PVA-Alginate and 0.5LAP:PVA-Alginate were 2.1±0.6% and 4.3±0.6%, respectively, which was below the acceptable limit (5%) (Zou et al., 2016). According to the ISO standard (ISO, 2002), our result confirmed that LAP: PVA-Alginate hydrogels could not result in severe hemolysis, which might be due to the hydrophilic nature of both PVA and alginate polymers. Therefore, LAP:PVA-Alginate might be a dressing construct with appropriate hemocompatibility.

Result of blood clotting test on the various samples is presented in Fig. 6C. This test reflects the alteration of antithrombogenic activity with increasing blood-sample contacting time. It was found that the absorption value of the hemolyzed blood solution in contact with all samples reduced with increasing time. However, the absorption value decreased at all time points for nanohybrid hydrogel groups compared to PVA-Alginate, suggesting that PVA-alginate had superior thromboresistant characteristic. Moreover, due to the lowest absorbance value of 2LAP:PVA-Alginate hydrogel at all time points, this nanohybrid hydrogel revealed the highest clotting activity. In order to compare the clotting times of various samples, the time at which the absorbance equals 0.1 is commonly described as the clotting time (Foruzanmehr, Hosainalipour,

Mirdamadi Tehrani, & Aghaeipour, 2014). It was discovered that increasing laponite content reduced the clotting time from 135 min (at PVA-Alginate) to less than 20 min (at 2LAP:PVA-alginate) which clearly confirmed that LAP:PVA-Alginate could encourage blood coagulation and had a appropriate hemostatic characteristic. The representative image of the 12-well plate consisting of various samples after contacting with whole blood for a specific time of 135 min (Fig. 6E) could also noticeably emphasize the earlier formation of a clot in the nanohybrid hydrogels. According to our results, while PVA-Alginate hydrogel could absorb the whole blood, they could not motivate the formation of clot on the surface of hydrogel. However, the addition of laponite nanoplatelets to PVA-alginate reduced blood clotting time, suggesting the role of laponite content on the denaturing of fibrinogen and clot activation. Fig. 6D schematically presents the effect of negatively charged laponite nanoplatelets on the clot formation. Generally, blood coagulation chemical cascade is a multi-step process at which clot is its final product. When blood interacts with negatively charged laponite nanoplatelets, intrinsic pathway of thrombosis initiated which triggers coagulation factors such as FXII in a few seconds and activates thrombin formation (Dawson & Oreffo, 2013). The formation of thrombin converts plasma fibrinogen to fibrin monomers which polymerize and crosslink to form a fibrous mesh which results in the formation of thrombosis (blood clot) (Shankarraman, Davis-Gorman, Copeland, Caplan, & McDonagh, 2012). Therefore, according to Fig. 6D, incorporation of laponite nanoplatelets as negatively charged components within hydrophilic hydrogel could accelerate the accumulation of clotting factors and support protein adsorption on the surface of hydrogels leading to dehydration of the injury site and consequently formation of blood clot (Jhong et al., 2014). Previous researches reported the role of negatively charged particles on the reducing the clotting time. For instance, Li *et al.* (C. Li et al., 2015) synthesized nanocomposite

hydrogel of acrylamide (AAm)-laponite-gelatin and showed that decrease in gelatin content and increase in laponite up to 2 wt.% resulted in the blood clot formation (C. Li et al., 2015).

According to our result, the novel LAP:PVA-Alginate nanohybrid hydrogel with adjustable mechanical, physical and biological properties and the significant capability to promote blood coagulation offers its durable hemostatic potential for wound healing application.

4. Conclusion

The aim of this study was to prepare novel nanohybrid hydrogels of LAP:PVA-Alginate and study the effects of laponite concentration on the physical, mechanical and biological properties of the hydrogels. Results confirmed that incorporation of laponite within the interpenetrating network of PVA-Alginate significantly reduced its swelling and degradation ratio and improved its mechanical properties. Moreover, it was found that LAP:PVA-Alginate nanohybrid hydrogels are nontoxic toward human fibroblast skin and MG63 cells. Blood-nanohybrid hydrogel interaction was assessed from the hemolysis test and kinetic clotting test. Results indicated that incorporation of laponite enhanced the hemolysis ratio of the hydrogels. Moreover, kinetic clotting test suggested an improved performance with increasing laponite content for blood coagulation. Our results suggest that LAP:PVA-Alginate hydrogel could be an ideal hydrogel for wound healing applications at the optimal concentration of laponite (0.5%) which will give proper swelling and degradation ratio with enhanced mechanical properties and blood coagulation activity.

Reference

Annabi, N., Nichol, J. W., Zhong, X., Ji, C., Koshy, S., Khademhosseini, A., & Dehghani, F. (2010). Controlling the porosity and microarchitecture of hydrogels for tissue engineering. *Tissue Engineering Part B: Reviews,* 16(4), 371-383.

Annabi, N., Tamayol, A., Uquillas, J. A., Akbari, M., Bertassoni, L. E., Cha, C., . . . Khademhosseini, A. (2014). 25th anniversary article: rational design and applications of hydrogels in regenerative medicine. *Advanced Materials,* 26(1), 85-124.

Arnaud, F., Parreno-Sadalan, D., Tomori, T., Delima, M. G., Teranishi, K., Carr, W., . . . McCarron, R. (2009). Comparison of 10 hemostatic dressings in a groin transection model in swine. *J Trauma,* 67(4), 848-855.

Auvray, L., & Lal, J. (1999). Interaction of polymer with clays. Argonne National Lab., IL (US).

Bowman, P. D., Wang, X., Meledeo, M. A., Dubick, M. A., & Kheirabadi, B. S. (2011). Toxicity of aluminum silicates used in hemostatic dressings toward human umbilical veins endothelial cells, HeLa cells, and RAW267. 4 mouse macrophages. *Journal of Trauma and Acute Care Surgery,* 71(3), 727-732.

Broderick, E., Lyons, H., Pembroke, T., Byrne, H., Murray, B., & Hall, M. (2006). The characterisation of a novel, covalently modified, amphiphilic alginate derivative, which retains gelling and non-toxic properties. *Journal of colloid and interface science,* 298(1), 154-161.

Cai, N., Li, C., Han, C., Luo, X., Shen, L., Xue, Y., & Yu, F. (2016). Tailoring mechanical and antibacterial properties of chitosan/gelatin nanofiber membranes with Fe 3 O 4 nanoparticles for potential wound dressing application. *Applied Surface Science,* 369, 492-500.

Cha, C., Shin, S. R., Gao, X., Annabi, N., Dokmeci, M. R., Tang, X. S., & Khademhosseini, A. (2014). Controlling mechanical properties of cell-laden hydrogels by covalent incorporation of graphene oxide. *Small,* 10(3), 514-523.

Darnell, M. C., Sun, J.-Y., Mehta, M., Johnson, C., Arany, P. R., Suo, Z., & Mooney, D. J. (2013). Performance and biocompatibility of extremely tough alginate/polyacrylamide hydrogels. *Biomaterials,* 34(33), 8042-8048.

Dawson, J. I., & Oreffo, R. O. (2013). Clay: new opportunities for tissue regeneration and biomaterial design. *Adv Mater,* 25(30), 4069-4086.

Du, J., Zhu, J., Wu, R., Xu, S., Tan, Y., & Wang, J. (2015). A facile approach to prepare strong poly (acrylic acid)/LAPONITE® ionic nanocomposite hydrogels at high clay concentrations. *RSC Advances,* 5(74), 60152-60160.

Eslahi, N., Simchi, A., Mehrjoo, M., Shokrgozar, M. A., & Bonakdar, S. (2016). Hybrid cross-linked hydrogels based on fibrous protein/block copolymers and layered silicate nanoparticles: tunable thermosensitivity, biodegradability and mechanical durability. *RSC Adv.,* 6(67), 62944-62957.

Foruzanmehr, M., Hosainalipour, S. M., Mirdamadi Tehrani, S., & Aghaeipour, M. (2014). Nano-structure TiO2 film coating on 316L stainless steel via sol-gel technique for blood compatibility improvement. *Nanomedicine Journal,* 1(3), 128-136.

Gaharwar, A. K., Avery, R. K., Assmann, A., Paul, A., McKinley, G. H., Khademhosseini, A., & Olsen, B. D. (2014). Shear-thinning nanocomposite hydrogels for the treatment of hemorrhage. *ACS nano,* 8(10), 9833-9842.

Gaharwar, A. K., Dammu, S. A., Canter, J. M., Wu, C.-J., & Schmidt, G. (2011). Highly extensible, tough, and elastomeric nanocomposite hydrogels from poly (ethylene glycol) and hydroxyapatite nanoparticles. *Biomacromolecules,* 12(5), 1641-1650.

Gaharwar, A. K., Rivera, C. P., Wu, C.-J., & Schmidt, G. (2011). Transparent, elastomeric and tough hydrogels from poly (ethylene glycol) and silicate nanoparticles. *Acta Biomater,* 7(12), 4139-4148.

Gaharwar, A. K., Schexnailder, P., Kaul, V., Akkus, O., Zakharov, D., Seifert, S., & Schmidt, G. (2010). Highly Extensible Bio‐Nanocomposite Films with Direction‐Dependent Properties. *Advanced Functional Materials,* 20(3), 429-436.

Golafshan, N., Gharibi, H., Kharaziha, M., & Fathi, M. (2017). A facile one-step strategy for development of a double network fibrous scaffold for nerve tissue engineering. *Biofabrication,* 9(2), 025008.

Golafshan, N., Kharaziha, M., & Fathi, M. (2016). Tough and conductive hybrid graphene-PVA: Alginate fibrous scaffolds for engineering neural construct. *Carbon*.

Guimarães, A. d. M. F., Ciminelli, V. S. T., & Vasconcelos, W. L. (2007). Surface modification of synthetic clay aimed at biomolecule adsorption: Synthesis and characterization. *Materials Research,* 10(1), 37-41.

Haraguchi, K., & Takehisa, T. (2002). Nanocomposite hydrogels: a unique organic-inorganic network structure with extraordinary mechanical, optical, and swelling/de-swelling properties. *Advanced Materials,* 14(16), 1120.

Hoare, T. R., & Kohane, D. S. (2008). Hydrogels in drug delivery: progress and challenges. *Polymer,* 49(8), 1993-2007.

Hoffman, A. S. (2012). Hydrogels for biomedical applications. *Advanced drug delivery reviews,* 64, 18-23.

Islam, M. S., & Karim, M. R. (2010). Fabrication and characterization of poly(vinyl alcohol)/alginate blend nanofibers by electrospinning method. *Colloids and Surfaces A: Physicochemical and Engineering Aspects,* 366(1-3), 135-140.

ISO, E. (2002). 10993. Biological evaluation of medical devices. Part 4: Selection of tests for interaction with blood. *Geneva, Switzerland*.

Jhong, J.-F., Venault, A., Liu, L., Zheng, J., Chen, S.-H., Higuchi, A., . . . Chang, Y. (2014). Introducing mixed-charge copolymers as wound dressing biomaterials. *ACS Appl Mater Interfaces,* 6(12), 9858-9870.

Jung, H., Kim, H.-M., Choy, Y. B., Hwang, S.-J., & Choy, J.-H. (2008). Itraconazole–Laponite: Kinetics and mechanism of drug release. *Applied Clay Science,* 40(1), 99-107.

Kamoun, E. A., Kenawy, E.-R. S., & Chen, X. (2017). A review on polymeric hydrogel membranes for wound dressing applications: PVA-based hydrogel dressings. *Journal of advanced research*.

Kharaziha, M., Shin, S. R., Nikkhah, M., Topkaya, S. N., Masoumi, N., Annabi, N., . . . Khademhosseini, A. (2014). Tough and flexible CNT–polymeric hybrid scaffolds for engineering cardiac constructs. *Biomaterials,* 35(26), 7346-7354.

Lee, K. Y., & Mooney, D. J. (2001). Hydrogels for tissue engineering. *Chemical reviews,* 101(7), 1869-1880.

Lee, K. Y., & Mooney, D. J. (2012). Alginate: properties and biomedical applications. *Progress in Polymer Science,* 37(1), 106-126.

Li, C., Mu, C., Lin, W., & Ngai, T. (2015). Gelatin Effects on the Physicochemical and Hemocompatible Properties of Gelatin/PAAm/Laponite Nanocomposite Hydrogels. *ACS Appl Mater Interfaces,* 7(33), 18732-18741.

Li, P., Kim, N. H., Hui, D., Rhee, K. Y., & Lee, J. H. (2009). Improved mechanical and swelling behavior of the composite hydrogels prepared by ionic monomer and acid-activated Laponite. *Applied Clay Science,* 46(4), 414-417.

Li, P., Kim, N. H., Yoo, G. H., & Lee, J. H. (2009). Poly (acrylamide/laponite) nanocomposite hydrogels: swelling and cationic dye adsorption properties. *Journal of Applied Polymer Science,* 111(4), 1786-1798.

Lin, H.-R., Ling, M.-H., & Lin, Y.-J. (2009). High strength and low friction of a PAA-alginate-silica hydrogel as potential material for artificial soft tissues. *Journal of Biomaterials Science, Polymer Edition,* 20(5-6), 637-652.

Liu, Y., Meng, H., Konst, S., Sarmiento, R., Rajachar, R., & Lee, B. P. (2014). Injectable dopamine-modified poly(ethylene glycol) nanocomposite hydrogel with enhanced adhesive property and bioactivity. *ACS Appl Mater Interfaces,* 6(19), 16982-16992.

Loizou, E., Butler, P., Porcar, L., Kesselman, E., Talmon, Y., Dundigalla, A., & Schmidt, G. (2005). Large scale structures in nanocomposite hydrogels. *Macromolecules,* 38(6), 2047-2049.

Mahdavinia, G. R., Ettehadi, S., Amini, M., & Sabzi, M. (2015). Synthesis and characterization of hydroxypropyl methylcellulose-g-poly (acrylamide)/LAPONITE® RD nanocomposites as novel magnetic-and pH-sensitive carriers for controlled drug release. *RSC Advances,* 5(55), 44516-44523.

Mahdavinia, G. R., Mousanezhad, S., Hosseinzadeh, H., Darvishi, F., & Sabzi, M. (2016). Magnetic hydrogel beads based on PVA/sodium alginate/laponite RD and studying their BSA adsorption. *Carbohydr Polym,* 147, 379-391.

Naficy, S., Kawakami, S., Sadegholvaad, S., Wakisaka, M., & Spinks, G. M. (2013). Mechanical properties of interpenetrating polymer network hydrogels based on hybrid ionically and covalently crosslinked networks. *Journal of Applied Polymer Science,* 130(4), 2504-2513.

Nair, S. H., Pawar, K. C., Jog, J. P., & Badiger, M. V. (2007). Swelling and mechanical behavior of modified poly (vinyl alcohol)/laponite nanocomposite membranes. *Journal of Applied Polymer Science,* 103(5), 2896-2903.

Nair, S. H., Pawar, K. C., Jog, J. P., & Badiger, M. V. (2007). Swelling and mechanical behavior of modified poly(vinyl alcohol)/laponite nanocomposite membranes. *Journal of Applied Polymer Science,* 103(5), 2896-2903.

Nie, L., Chen, D., Suo, J., Zou, P., Feng, S., Yang, Q., . . . Ye, S. (2012). Physicochemical characterization and biocompatibility in vitro of biphasic calcium phosphate/polyvinyl alcohol scaffolds prepared by freeze-drying method for bone tissue engineering applications. *Colloids and Surfaces B: Biointerfaces,* 100, 169-176.

Orive, G., Tam, S. K., Pedraz, J. L., & Hallé, J.-P. (2006). Biocompatibility of alginate–poly-l-lysine microcapsules for cell therapy. *Biomaterials,* 27(20), 3691-3700.

Pacelli, S., Paolicelli, P., Moretti, G., Petralito, S., Di Giacomo, S., Vitalone, A., & Casadei, M. A. (2016). Gellan gum methacrylate and laponite as an innovative nanocomposite hydrogel for biomedical applications. *European Polymer Journal,* 77, 114-123.

Riedinger, A., Pernia Leal, M., Deka, S. R., George, C., Franchini, I. R., Falqui, A., . . . Pellegrino, T. (2011). “Nanohybrids” based on pH-responsive hydrogels and inorganic nanoparticles for drug delivery and sensor applications. *Nano letters,* 11(8), 3136-3141.

Roozbahani, M., Kharaziha, M., & Emadi, R. (2017). pH Sensitive Dexamethasone Encapsulated Laponite Nanoplatelets: Release Mechanism and Cytotoxicity. *International journal of pharmaceutics*.

Shalumon, K. T., Anulekha, K. H., Nair, S. V., Nair, S. V., Chennazhi, K. P., & Jayakumar, R. (2011). Sodium alginate/poly(vinyl alcohol)/nano ZnO composite nanofibers for antibacterial wound dressings. *Int J Biol Macromol,* 49(3), 247-254.

Shankarraman, V., Davis‐Gorman, G., Copeland, J. G., Caplan, M. R., & McDonagh, P. F. (2012). Standardized methods to quantify thrombogenicity of blood‐contacting materials via thromboelastography. *Journal of Biomedical Materials Research Part B: Applied Biomaterials,* 100(1), 230-238.

Sharifi, S., Blanquer, S. B., van Kooten, T. G., & Grijpma, D. W. (2012). Biodegradable nanocomposite hydrogel structures with enhanced mechanical properties prepared by photo-crosslinking solutions of poly (trimethylene carbonate)–poly (ethylene glycol)–poly (trimethylene carbonate) macromonomers and nanoclay particles. *Acta biomaterialia,* 8(12), 4233-4243.

Tanaka, Y., Gong, J. P., & Osada, Y. (2005). Novel hydrogels with excellent mechanical performance. *Progress in Polymer Science,* 30(1), 1-9.

Tarun, K., & Gobi, N. (2012). Calcium alginate/PVA blended nano fibre matrix for wound dressing. *Indian J. Fibre Text. Res,* 37, 127-132.

Thankam, F. G., Muthu, J., Sankar, V., & Gopal, R. K. (2013). Growth and survival of cells in biosynthetic poly vinyl alcohol–alginate IPN hydrogels for cardiac applications. *Colloids and Surfaces B: Biointerfaces,* 107, 137-145.

Thomas, L. V., Arun, U., Remya, S., & Nair, P. D. (2009). A biodegradable and biocompatible PVA–citric acid polyester with potential applications as matrix for vascular tissue engineering. *Journal of Materials Science: Materials in Medicine,* 20(1), 259.

Thomas, S. (1997). Assessment and management of wound exudate. *Journal of wound care,* 6(7), 327.

Vogler, E. A. (2012). Protein adsorption in three dimensions. *Biomaterials,* 33(5), 1201-1237.

Vu, L. T., Jain, G., Veres, B. D., & Rajagopalan, P. (2014). Cell migration on planar and three-dimensional matrices: a hydrogel-based perspective. *Tissue Engineering Part B: Reviews,* 21(1), 67-74.

Wang, S., Zheng, F., Huang, Y., Fang, Y., Shen, M., Zhu, M., & Shi, X. (2012). Encapsulation of amoxicillin within laponite-doped poly (lactic-co-glycolic acid) nanofibers: preparation, characterization, and antibacterial activity. *ACS Appl Mater Interfaces,* 4(11), 6393-6401.

Wong, M. (2004). Alginates in tissue engineering. *Biopolymer methods in tissue engineering*, 77-86.

Wu, C.-J., Gaharwar, A. K., Chan, B. K., & Schmidt, G. (2011). Mechanically tough pluronic F127/laponite nanocomposite hydrogels from covalently and physically cross-linked networks. *Macromolecules,* 44(20), 8215-8224.

Wu, C.-J., Gaharwar, A. K., Schexnailder, P. J., & Schmidt, G. (2010). Development of biomedical polymer-silicate nanocomposites: a materials science perspective. *Materials,* 3(5), 2986-3005.

Xu, L.-C., Bauer, J. W., & Siedlecki, C. A. (2014). Proteins, platelets, and blood coagulation at biomaterial interfaces. *Colloids and Surfaces B: Biointerfaces,* 124, 49-68.

Yang, H., Hua, S., Wang, W., & Wang, A. (2011). Composite hydrogel beads based on chitosan and laponite: preparation, swelling, and drug release behaviour. *Iran Polym J,* 20(6), 479-490.

Yang, J., Zhu, L., Yan, X., Wei, D., Qin, G., Liu, B., . . . Chen, Q. (2016). Hybrid nanocomposite hydrogels with high strength and excellent self-recovery performance. *RSC Advances,* 6(64), 59131-59140.

Zou, Y.-H., Zeng, R.-C., Wang, Q.-Z., Liu, L.-J., Xu, Q.-Q., Wang, C., & Liu, Z.-W. (2016). Blood compatibility of zinc–calcium phosphate conversion coating on Mg–1.33Li–0.6Ca alloy. *Frontiers of Materials Science,* 10(3), 281-289.

Figure Caption

Fig. 1. Synthesis of LAP:PVA-Alginate nanohybrid hydrogel: (A) Schematic representation for the fabrication of LAP:PVA-Alginate nanohybrid hydrogels. (B) FTIR spectra of laponite, PVA, alginate, PVA-Alginate and 2LAP:PVA-Alginate nanohybrid hydrogel. (C) TEM image of laponite nanoplates. (D) XRD patterns of laponite, PVA, alginate, PVA-Alginate and 2LAP:PVA-Alginate nanohybrid hydrogels.

Fig. 2 SEM micrographs of LAP:PVA-Alginate with containing various laponite contents. While laponite nanoplatelets were uniformly distributed within 0.5LAP:PVA-Alginate nanohybrid hydrogel, agglomeration of laponite nanoplatelets could be detected at 1Laponite:PVA-Alginate and 2LAP:PVA-Alginate hydrogels. High magnification SEM images show the distribution of laponite nanoplatelets.

Fig. 3. (A) Swelling ratio and (B) degradation rate of nanohybrid hydrogels as a function of laponite content. A strong correlation between laponite concentration and swelling degree/degradation rate could be detected attributing to the role of laponite nanoplatelets as the secondary crosslinker for polymers network.

Fig. 4 Effect of laponite nanoplatelets on the mechanical properties of the hydrogels; (A) Representative stress-strain curves of hydrogels at wet condition. (B) Elongation, (C) toughness, (D) strength, and (E) tensile modulus of the hydrogels as a function of laponite content (*$P<0.05$). (F) The schematic showing the role of crosslinking process of alginate and PVA as well as laponite nanoplatelets on the mechanical properties of nanohybrid hydrogels.

Fig. 5. The viability of A) human fibroblast skin and (B) MG63 cell lines seeded on the hydrogels for various times, as a function of laponite content measured using MTT assays (The absorbance was normalized against the control (TCP) at each time interval (* $P<0.05$).

Fig. 6. Effect of hydrogels on the blood interaction: (A) Amounts of adsorbed BSA on the hydrogels as a function of laponite content. (B) Hemolysis ratio of the hydrogels as a function of laponite content (* $P<0.05$). (C) Kinetic clotting curves plotted as a function of time and nanohybrid composition. (D) The schematic indicating the thrombogenic potential of laponite and its role on the blood coagulation cascade. Laponite affects the blood coagulation via absorption of water molecules and proteins to its surface to activate intrinsic coagulation pathway. The interactions result in concentrating the blood cells and clotting factors and promoting hemostasis. (E) Effect of laponite concentration on the blood clotting.

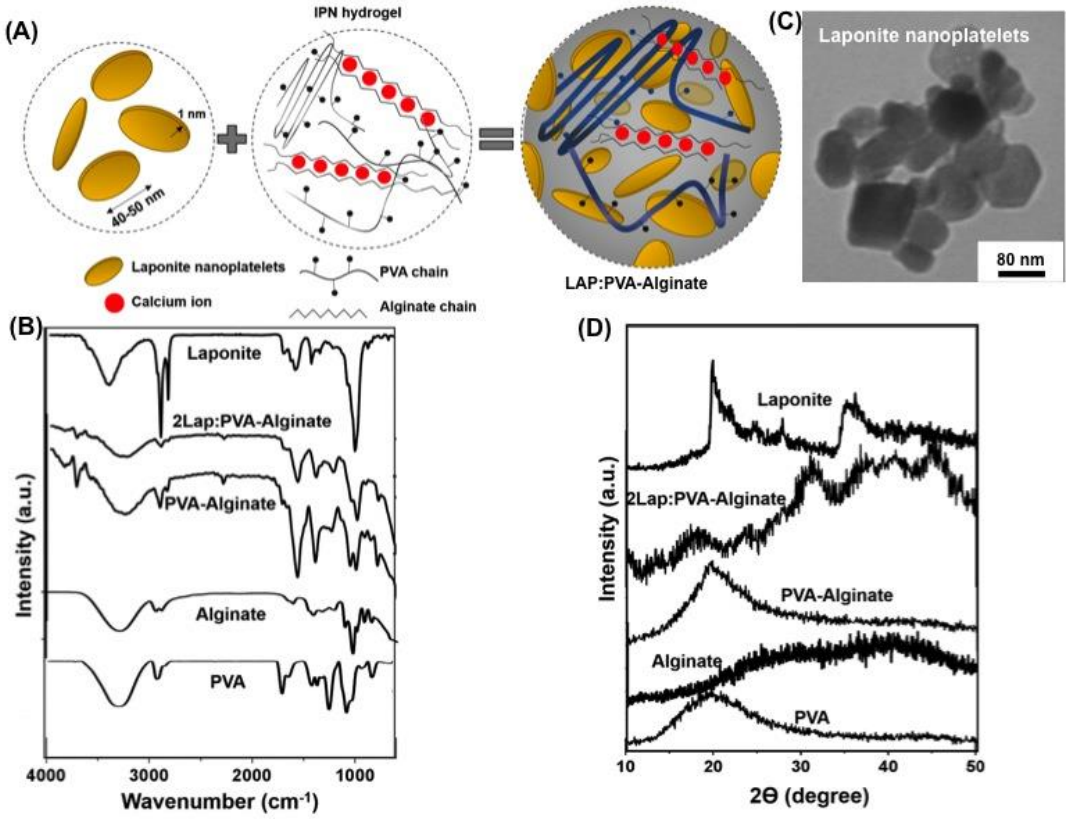

Fig. 1. Synthesis of LAP:PVA-Alginate nanohybrid hydrogel: (A) Schematic representation for the fabrication of LAP:PVA-Alginate nanohybrid hydrogels. (B) FTIR spectra of laponite, PVA, alginate, PVA-Alginate and 2LAP:PVA-Alginate nanohybrid hydrogel. (C) TEM image of laponite nanoplates. (D) XRD patterns of laponite, PVA, alginate, PVA-Alginate and 2LAP:PVA-Alginate nanohybrid hydrogels.

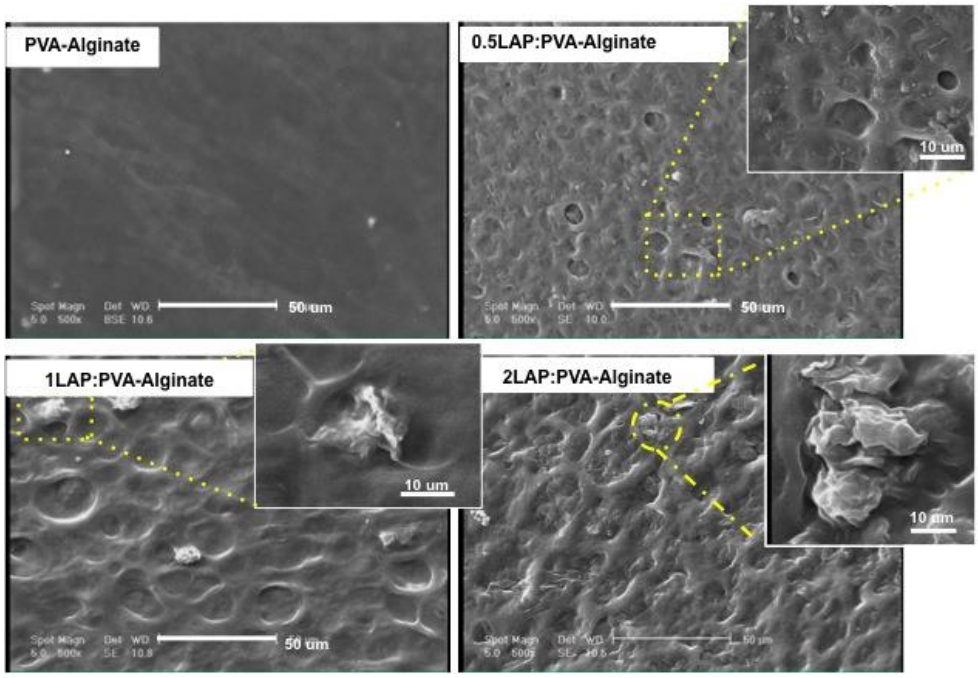

Fig. 2 SEM images of LAP:PVA-Alginate containing various amounts of laponite. While laponite nanoplatelets uniformly distributed within 0.5LAP:PVA-Alginate nanohybrid hydrogel, agglomeration of laponite nanoplatelets is detected at 1LAP:PVA-Alginate and 2LAP:PVA-Alginate hydrogels. High magnification SEM images show the distribution of laponite nanoplatelets.

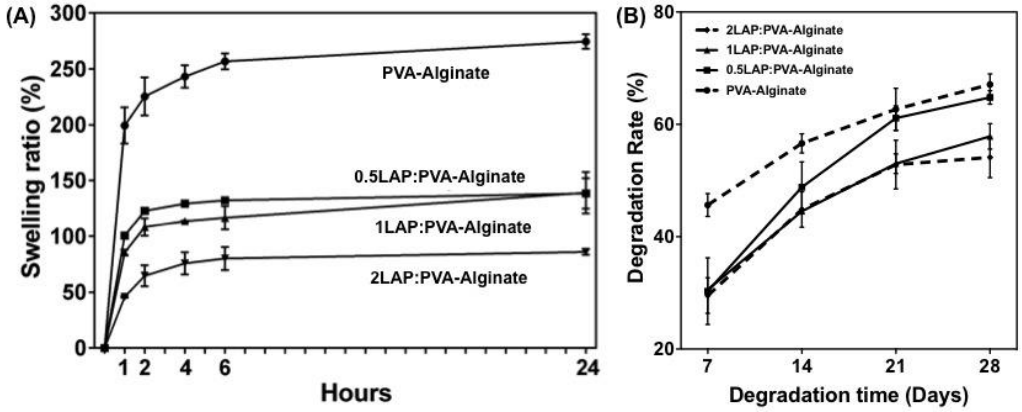

Fig. 3. (A) Swelling ratio and (B) degradation rate of nanohybrid hydrogels as a function of laponite content. A strong correlation between laponite concentration and swelling degree/degradation rate could

be detected attributing to the role of laponite nanoplatelets as the secondary crosslinker for polymers network.

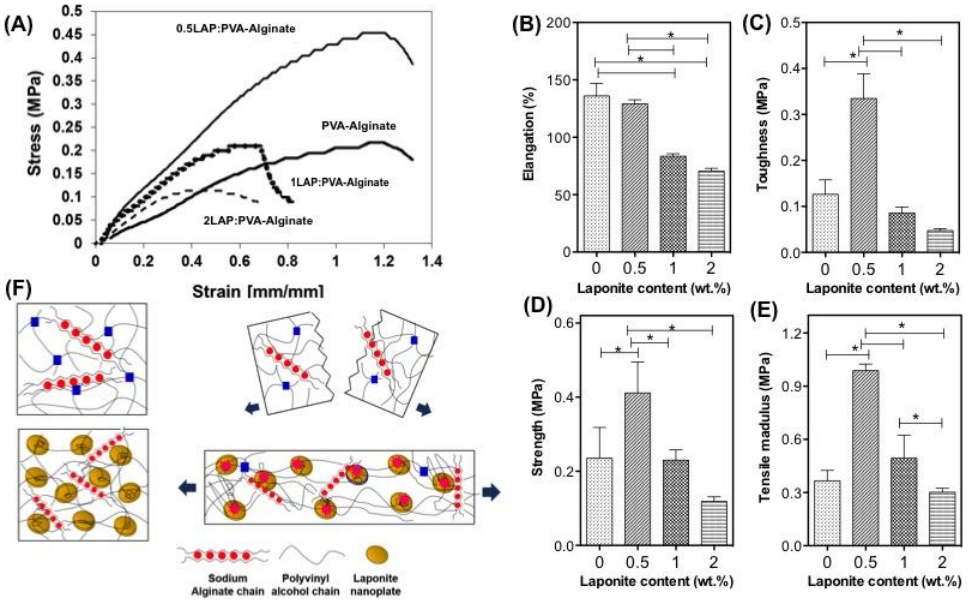

Fig. 4 Effect of laponite nanoplatelets on the mechanical properties of the hydrogels; (A) Representative stress-strain curves of hydrogels at wet condition. (B) Elongation, (C) toughness, (D) strength, and (E) tensile modulus of the hydrogels as a function of laponite content (*P<0.05). (F) The schematic showing the role of crosslinking process of alginate and PVA as well as laponite nanoplatelets on the mechanical properties of nanohybrid hydrogels.

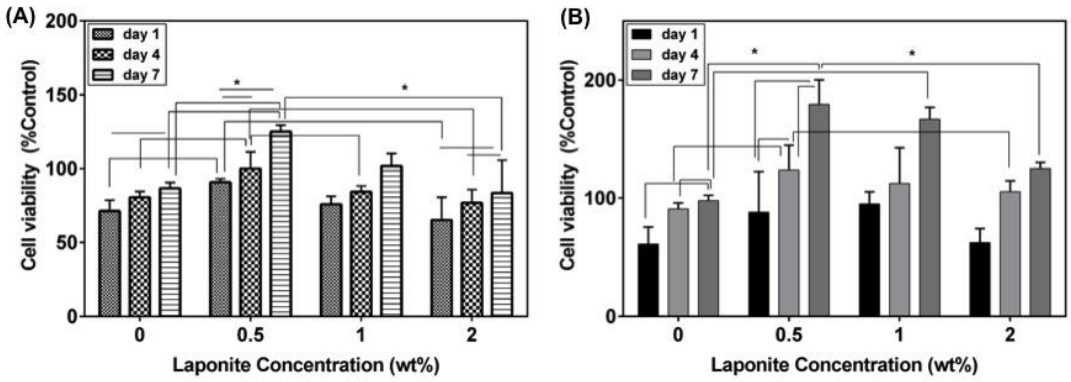

Fig. 5. The viability of A) human fibroblast skin and (B) MG63 cell lines seeded on the hydrogels for

various times, as a function of laponite content measured using MTT assays (The absorbance was normalized against the control (TCP) at each time interval (* P<0.05).

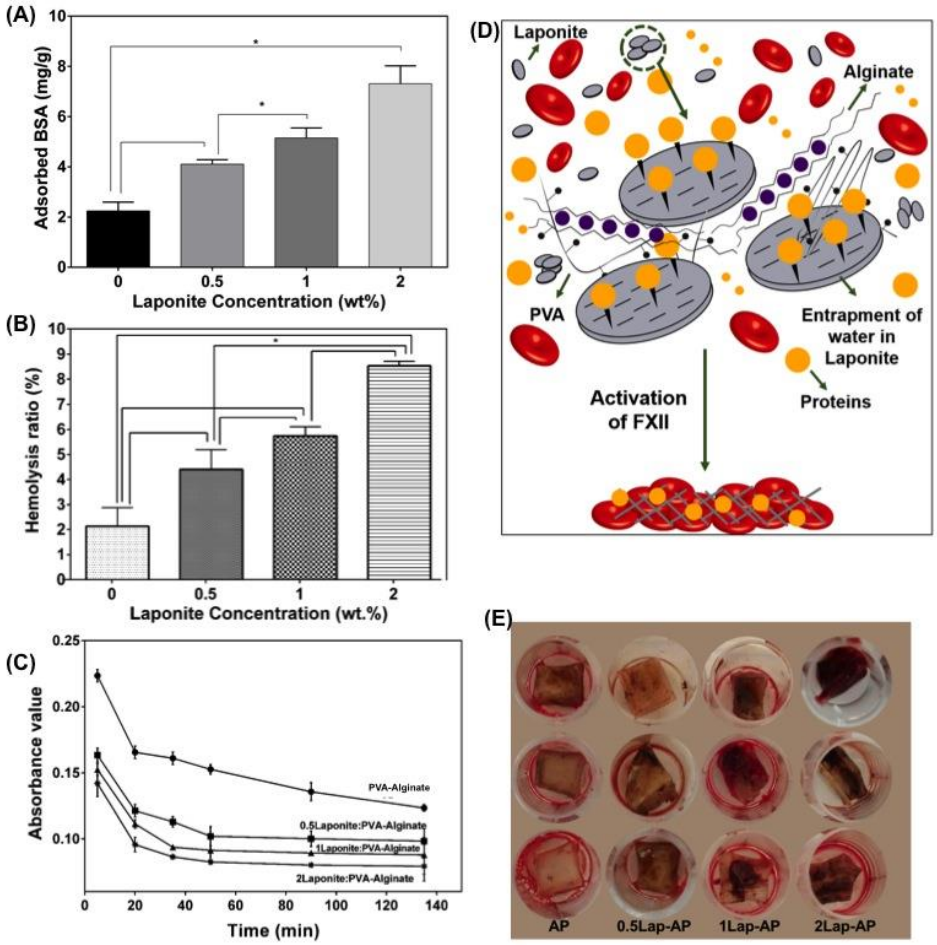

Fig. 6. Effect of hydrogels on the blood interaction: (A) Amounts of adsorbed BSA on the hydrogels as a function of laponite content. (B) Hemolysis ratio of the hydrogels as a function of laponite content (* P<0.05). (C) Kinetic clotting curves plotted as a function of time and nanohybrid composition. (D) The schematic indicating the thrombogenic potential of laponite and its role on the blood coagulation cascade. Laponite affects the blood coagulation via absorption of water molecules and proteins to its surface to activate intrinsic coagulation pathway. The interactions result in concentrating the blood cells and clotting factors and promoting hemostasis. (E) Effect of laponite concentration on the blood clotting.